

Insight into $K^*(892)^0$ production in pp collisions as a function of collision energy, event-topology, and multiplicity with ALICE at the LHC

Rutuparna Rath^{a,*}

^a*Department of Physics, Indian Institute of Technology Indore,
Simrol, Indore-453552, India,
(For the ALICE collaboration)*

E-mail: rutuparna.rath@cern.ch

Hadronic resonances are short-lived particles whose lifetimes are comparable to the hadronic phase lifetime of the system produced in ultra-relativistic nucleon-nucleon or nuclear collisions. These resonances are sensitive to the hadronic phase effects such as re-scattering and regeneration processes which might affect the resonance yields and shape of the transverse momentum spectra. In addition, event shape observables like transverse sphericity are sensitive to the hard and soft processes and they represent a useful tool to separate the isotropic from jetty-dominated events in proton–proton (pp) collisions. A double differential study of transverse sphericity and multiplicity allows us to understand the resonance production mechanism with event topology and system size, respectively. Furthermore, the measurements in small systems are used as a reference for heavy-ion collisions and are helpful for the tuning of Quantum Chromodynamics (QCD) inspired event generators. In this proceeding, we present recent results on $K^*(892)^0$ obtained by the ALICE Collaboration in pp collisions at several collision energies, event multiplicities, and as a function of transverse sphericity. The results include the transverse momentum spectra, yields, and their ratio to long-lived particles. The measurements are compared with model predictions from PYTHIA8, EPOS-LHC, and DIPSY.

*The Ninth Annual Conference on Large Hadron Collider Physics - LHCP2021
7-12 June 2021
Online*

*Speaker

1. Introduction

The resonance particles are short-lived hadrons having a lifetime comparable to the hadronic phase produced in the ultra-relativistic heavy-ion collisions. Therefore, resonances are sensitive to the hadronic phase effects such as rescattering and regeneration processes (see Fig. 1) which might affect the resonance yields and the shape of the transverse momentum spectra.

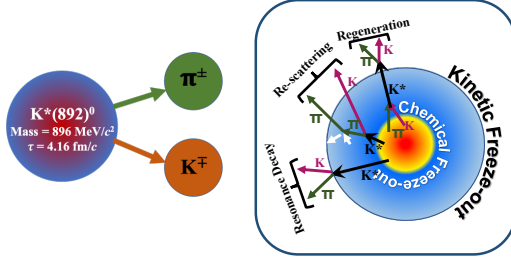


Figure 1: Pictorial view of the highest branching ratio decay of $K^*(892)^0$ (left) and of the different physics processes of resonances in the hadronic phase (right).

The $K^*(892)^0$ is a vector meson with a comparable mass to the $\phi(1020)$ but differs in strangeness quark content by one unit. The study of the production of these resonances in high energy collisions, hence, may shed light on understanding the strangeness production dynamics. Historically, the results from small collision systems are used as a baseline to understand the particle production in heavy-ion collisions. However, the enhanced strangeness production and long-range azimuthal correlation in high-multiplicity pp collisions at the LHC energies [1, 2] show similar behavior as observed in heavy-ion collisions. Such results in small collision systems can not be reproduced qualitatively by most of the QCD based Monte Carlo (MC) models. Thus, the similarities and the differences between pp, p–Pb, and Pb–Pb collisions are not fully understood yet. One of the major issues of getting a clear picture is related to the selection bias and autocorrelation effects observed in the results of different collision systems. To understand which is the particle production mechanism, it is necessary to separate the events originating from soft scattering processes (Underlying Events-UE) from those originating from hard parton–parton scattering. The major contribution to UE comes from the multi-partonic interactions (MPIs), initial and final state radiation, and beam-beam remnants. The study of UE becomes more important at the LHC energies where we see the dominance of MPIs with multiplicity [3]. Essentially all high-multiplicity collisions are dominated by the underlying event and hard events are rare. Hence, it is fundamental to understand whether the particle production is originated by the product of many small parton–parton collisions or if there is a significant contribution due to violent single parton–parton scattering. In order to do so, it is possible to disentangle events dominated by the soft from the those dominated by hard QCD processes using the transverse sphericity (S_0). S_0 for an event is defined as

$$S_0^{p_{T=1}} = \frac{\pi^2}{4} \left(\frac{\sum_i |\vec{p}_{T_i} \times \hat{n}|}{\sum_i p_{T_i}} \right)^2. \quad (1)$$

Here “ \hat{n} ” is chosen in such a way to minimize the S_0 value for an event. The back-to-back jet structure leads to a S_0 value towards 0, while, for events dominated by the soft processes, the azimuthal distribution of particles becomes isotropic and S_0 value approaches one. In this study, the selection of the jetty (isotropic) events are defined as the bottom (top) 20% events of the $S_0^{p_{T=1}}$ distribution.

2. Results and discussion

The measurements of K^{*0} meson production have been performed in pp collisions at $\sqrt{s} = 13$ TeV recorded by ALICE during LHC Run 2. The transverse sphericity distribution for pp collisions at $\sqrt{s} = 13$ TeV events are shown in Fig. 2 for different multiplicity classes as shown in the legend.

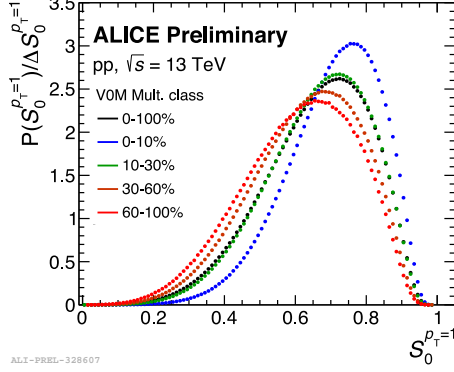


Figure 2: Transverse sphericity distribution in pp collisions at $\sqrt{s} = 13$ TeV for different V0M multiplicity classes as shown in the legend.

The K^{*0} is reconstructed through invariant mass technique from its hadronic decay with the largest branching ratios (BR): $K^{*0} \rightarrow \pi^{\pm}K^{\mp}$ (66.6%). The uncorrelated background is estimated using the event-mixing method from the invariant mass distribution of unlike-sign $K\pi$ combinations from different events. This combinatorial background is subtracted from the unlike-sign invariant mass distribution in each p_T bin. The resulting distribution is fitted with a combined function of a Breit-Wigner (to describe the resonance) and a 2^{nd} order polynomial (to describe the residual background). An example of the fit is shown in Fig. 3.

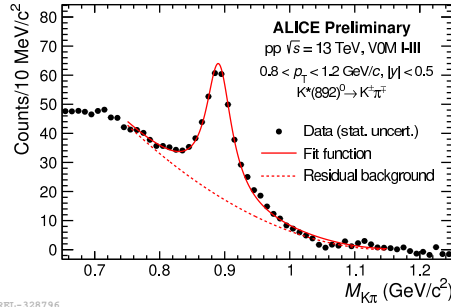


Figure 3: Fit to the invariant mass distribution obtained from $\pi^{\pm}K^{\mp}$ pairs after the mixed event combinatorial background subtraction for events in the (0 – 10)% V0M multiplicity class and integrated in S_0 .

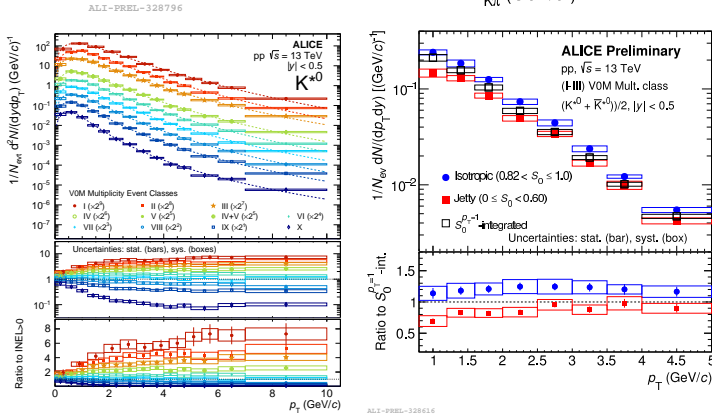


Figure 4: (Left) K^{*0} transverse momentum spectra obtained in different multiplicity classes using the V0M estimator for pp collisions at $\sqrt{s} = 13$ TeV [5]. (Right) K^{*0} transverse momentum spectra obtained in the 0–10% V0M multiplicity interval for pp collisions at $\sqrt{s} = 13$ TeV for all the three sphericity classes considered in this analysis.

2.1 K^{*0} p_T -spectra

Figure 4 (left) shows the K^{*0} p_T -spectra for different multiplicity intervals. The evolution of spectral shape with multiplicity for $p_T < 5$ GeV/c is consistent with the presence of radial flow.

On the other hand, for $p_T > 5$ GeV/c the spectral shape is similar across multiplicity. Figure 4 (right) shows the p_T -spectra in the 0–10% multiplicity interval using the VOM estimator [4] for pp collisions at $\sqrt{s} = 13$ TeV for all the three sphericity classes considered in this analysis. The p_T -spectra is obtained as a function of S_0 for K^{*0} by considering the top (bottom) 20% sphericity selection to separate isotropic (jetty) events. We observe a separation of the p_T -spectra for isotropic and jetty events with weak (if any) dependence on p_T . In addition, more K^{*0} are produced in isotropic events than jetty ones.

2.2 Particle ratio

Ratios of p_T -integrated particle yields K^{*0}/K , ϕ/K , and Ξ/ϕ as functions of charged-particle density $\langle dN_{ch}/d\eta \rangle_{|\eta| < 0.5}$ in pp collisions at $\sqrt{s} = 13$ TeV are shown in Fig. 5. To study the energy and system size dependence of these ratios, they are compared with the available results for different collisions system like pp at $\sqrt{s} = 7$ TeV, p–Pb collisions at $\sqrt{s_{NN}} = 5.02$ TeV, and Pb–Pb at $\sqrt{s_{NN}} = 2.76$ TeV as indicated in the legend. It is clear from this figure that K^{*0}/K ratio does not depend on collision energy and system size, since the results obtained in pp and p–Pb collisions are consistent at similar multiplicities. A suppression in the K^{*0}/K ratio as a function of multiplicity is observed. This might be an indication of the possible formation of hadron gas phase in high-multiplicity pp collisions. For ϕ meson, which has a larger lifetime compared to the K^{*0} one, the ratio with respect to K shows a fairly constant behavior as a function of charged-particle density. The Ξ/ϕ ratio increases in the low-multiplicity region, and becomes almost constant at high-multiplicities. The decrease of the Ξ/ϕ ratio with decreasing multiplicity can be attributed to the canonical suppression of Ξ in small systems.

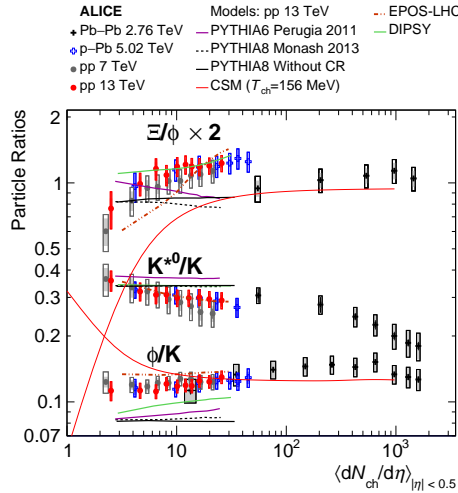


Figure 5: Ratios of p_T -integrated particle yields K^{*0}/K , ϕ/K , and Ξ/ϕ in pp collisions at $\sqrt{s} = 13$ TeV as functions of $\langle dN_{ch}/d\eta \rangle_{|\eta| < 0.5}$ [4, 6]. These measurements are compared with data from pp collisions at $\sqrt{s} = 7$ TeV [7], p–Pb collisions at $\sqrt{s_{NN}} = 5.02$ TeV [8, 9], and Pb–Pb collisions at $\sqrt{s_{NN}} = 2.76$ TeV [10, 11], as well as results from common event generators [12–15] and a Canonical Statistical Model calculation [5].

3. Summary

The large data sample collected by the ALICE allows us to study the energy, multiplicity, and sphericity dependence of resonance production. The hardening of the p_T -spectra with charged particle multiplicity in pp collisions indicate the presence of radial flow effect. Moreover, K^{*0} p_T -spectra as a function of transverse sphericity classes show higher production of resonances in isotropic events compared to jetty ones. The K^{*0}/K ratio is independent of collision system and energy for a given multiplicity value. The suppression of K^{*0}/K ratio in high-multiplicity pp collisions supports the possible presence of hadronic gas phase in small systems.

References

- [1] J. Adam *et al.* [ALICE Collaboration]: Nature Phys. **13**, 535 (2017).
- [2] V. Khachatryan *et al.* [CMS Collaboration], JHEP **09**, 091 (2010).
- [3] A. Khuntia, S. Tripathy, A. Bisht and R. Sahoo, J. Phys. G **48**, 035102 (2021).
- [4] S. Acharya *et al.* [ALICE], Eur. Phys. J. C **80**, 167 (2020).
- [5] S. Acharya *et al.* [ALICE], Phys. Lett. B **807**, 135501 (2020).
- [6] S. Acharya *et al.* [ALICE], Eur. Phys. J. C **80**, 693 (2020).
- [7] S. Acharya *et al.* [ALICE], Phys. Rev. C **99**, 024906 (2019).
- [8] J. Adam *et al.* [ALICE], Eur. Phys. J. C **76**, 245 (2016).
- [9] J. Adam *et al.* [ALICE], Phys. Lett. B **758**, 389 (2016).
- [10] B. B. Abelev *et al.* [ALICE], Phys. Rev. C **91**, 024609 (2015).
- [11] J. Adam *et al.* [ALICE], Phys. Rev. C **95**, 064606 (2017).
- [12] C. Flensburg, G. Gustafson and L. Lonnblad, JHEP **08**, 103 (2011).
- [13] T. Pierog, I. Karpenko, J. M. Katzy, E. Yatsenko and K. Werner, Phys. Rev. C **92**, 034906 (2015).
- [14] P. Z. Skands, Phys. Rev. D **82**, 074018 (2010).
- [15] P. Skands, S. Carrazza and J. Rojo, Eur. Phys. J. C **74**, 3024 (2014).